Effect of Water Radiolysis on Corrosion: Steel, Cobalt and Nickel Alloys

A.Y. Musa, M. Behazin, Q.W. Knapp, D. Mizzi, J.C. Wren
Department of Chemistry, Western University
London, ON, N6A 5B7, Canada
(jcwren@uwo.ca)

Abstract

Steel, cobalt and nickel alloysare used in the coolant system (or primary heat transport system) of a nuclear power plant. To understand the effect of γ-radiation on the corrosion mechanism of these alloys, a combination of electrochemical measurements and surfaceanalyses as a function of the water chemistry, with and without γ-radiation present, were performed.Results to date have shown that γ-radiation has a major impact on the corrosion process by changing the corrosion potential in a system. This determines the nature of the oxide phase (chemical state and morphology) that forms on a corroding alloy surface.

1. Introduction

A number of different alloys are used in the coolant system (or primary heat transport system) of a nuclear power plant. The piping and main fittings are made of steel alloys, the heat exchangers (or steam generators) use nickel alloys for their tubing, and special components (such as valve facings) use hard cobalt alloys [1–3]. The effects of the metallurgical propertiesof these alloyson corrosion have been well studied. However, less research has been done on the effect of aqueous chemistry on the corrosion behaviour of these alloys. Because of the number of different alloys that contact the coolant and the radiation fields that are present, the corrosion environment in a nuclear reactor coolant system deserves some extra attention. Uniform corrosion is the main source of metallic impurities in the coolant and their accumulation can lead to the formation of insoluble solids, typically called 'crud' (Chalk River unidentified deposit). In the reactor corestable isotopescan absorb a neutron and potentially become radioactive (e.g., to form ^{54}Mn, ^{58}Co, ^{59}Fe, ^{60}Co, ^{63}Ni) [4–6]. Temporary deposition of 'crud' in the reactor core can promote this neutron activation. Transport in the coolant and deposition of radioactivematerials on coolant system components outside the biological shielding of the reactorcore creates a potential source of radiation exposure for plant workers. Therefore, understanding the factors influencing the corrosion of metal alloys is important for the safe and optimal operation of nuclear power plants.

The radiolysis of water produces highly reactive radicals ($\bullet$OH, $\bullet$H, $\bullet e_{aq}^-$, $\bullet HO_2$ and $\bullet O_2^-$) and molecular species (H_2, O_2 and H_2O_2) that affect the reduction-oxidation (redox) chemistry in water that controls corrosion [7]. Additionally, there iscomplex chemistry that occurs between dissolved metal ions and water radiolysis products. Together, water radiolysis and metal ion reactions affect the nature of the oxidefilm forms on the metal alloys in the reactor coolant system.

We are conducting a systematic study of oxide film formation and conversion to other oxides on stainless steel, carbon steel, a cobalt alloy and a nickel alloy under chemical environments relevant to their use in a nuclear power plant.The oxide formation on these surfaces has been investigated as a function of pH, temperature, electrolyte concentration and the concentration of dissolved additives such as H_2O_2, O_2 and ferrous ion under both unirradiated and irradiated conditions. A range of electrochemical measurements and ex-situ surface analyses have been used to obtain a complete picture of corrosion processes occurring on these surfaces. Many of the individual studies on oxide formation on these surfaces have been published [1–3,8].

In this work, we compare the effects of γ-radiation on water chemistry and the oxidation processes occurring on carbon steel, Type 316L stainless steel, Stellite-6 (a cobalt-based alloy) and Inconel 600 (a nickel-based alloy) at pH_{25^oC} 10.6 and at different temperatures (25 and 80 ^{0}C). We highlight the similarities and differences in the way in which ionizing radiation affects corrosion of these metals. We studythe corrosion behaviour of these alloys at pH_{25^oC} 10.6 because this is near the pHof the coolant water of a CANDU-typenuclear reactor.This pH is chosen to minimize the corrosion of the carbon steel that makes up most of the coolant system as the solubilities of Fe^{II}, Co^{II} and Ni^{II}oxides are at a minimum near this pH. The corrosion of these alloys at pHsnear 10 is significantly different from the behaviour seen at lower pHs.

2. Experimental

The alloys used in this study were Type AISI 316L stainless steel, Grade A516 Gr70 carbon steel, Stellite-6 and Inconel 600. The stainless steel(SS) and Inconel 600 were purchased from Goodfellow while the Stellite-6 and carbon steel (CS)werepurchased from Metal Samples Company. The alloy compositions provided by the manufacturers are listed in Table 1.

Table 1: Alloy compositions (wt%) used in this study

Alloy	Fe	Co	Cr	Ni	Minor elements
SS	Balance	–	18	10	Mo (3), C (0.03), Mn (1), Si (0.75)
CS	Balance	–	–	–	C (0.23), Mn (1.05), Si (0.22)
Stellite-6	2.92	Balance	27.62	2.62	Mo (0.41), C (1.42), Mn (0.27), Si (1.07), W (4.07)
Inconel 600	8	–	15	Balance	Mn (1)

The electrochemical measurements were performed in a three-electrode electrochemical cell with the alloy of interest as the working electrode (WE), a Pt mesh (Alfa Aesar, 99.9% purity) as the counter electrode (CE), and a reference electrode (RE). Detailed descriptions of the electrochemical cell, electrode and electrolyte preparation, instrumentation, and data acquisition and analysis can be found elsewhere [1–3]. The electrochemical analyses included corrosion potential measurement, cyclic voltammetry, and current and electrochemical impedance spectroscopy (EIS) measurements during long-term potentiostatic polarization.

Irradiation experiments were conducted in a γ-cell (MDS Nordion Gammacell 220 Excel Cobalt-60 irradiator). The electrochemical cell was positioned inside the γ-cell sample chamber and the chamber was lowered into the γ-cell irradiation zone (which consisted of 11 tubular pencils containing ^{60}Co). The radiation dose rate during the period of the experiments ranged from 4.3 to 5.5 kGy h^{-1} (1 Gy is 1 Jkg^{-1} absorbed energy).Higher temperature corrosion tests (150 ^{0}C) were performed with a test coupon contained in a 20 ml sealed vial. The sealed vials were placed inside an autoclave (250 mL Type 316 stainless steel pressure vessel (Parr Instrument Company, model 4760)) and the autoclave was filled with water to provide a pressure balance on the vials when heated.The autoclave was located inside an electrical heating sleeve and placed inside the γ-cell. Upon termination of an experiment the electrode or coupon surface wasexamined using scanning electron microscopy (SEM), x-ray photoelectron spectroscopy (XPS), Auger electron spectroscopy (AES) and Raman spectroscopy. Detailed descriptions of the sample preparation, analysis techniques and methodologies can be found in references [1–3]. The experiments that are discussed below were all conducted in Ar-purged 0.01 M borate buffer solutions adjusted to pH 10.6 by addition of an NaOH solution.

3. Results and Discussion

3.1 Corrosion Potential

Fig. 1 compares the corrosion potential, E_{CORR}, recorded on the four different alloys during corrosion in a deaerated 10 mM borate solution with and without irradiation. The steady-state E_{CORR} values on all of the alloys increase substantially when the corroding system is exposed to γ-radiation. The time required for the systems to reach a steady-state value for E_{CORR} varied, but in all cases, steady-state was achieved within ~24 h.

Our previous studies on carbon steel have established that γ-radiation affects the corrosion process primarily by producing redox activeH_2O_2 in the aqueous phase [9]. Aqueous corrosion involves the oxidation of metal species coupled with the reduction of aqueous species. On a naturally corroding surface, when no external polarization is applied, the net rates of oxidation and reduction must be equal to maintain charge and mass balances. An increase in the concentration of H_2O_2 in the water caused by water radiolysis increases the rate of the reduction half reaction, and to maintain the charge and mass balances, the metal oxidation rate also increases. This results in an increase in E_{CORR}. Indeed we were able to simulate the increase in E_{CORR} due to γ-radiation on all of the surfaces by the addition of an appropriate concentration of $H_2O_2$to the cell electrolyte solutions [9].

We have not performed E_{CORR} measurements as a function of radiation dose rate. However, we have established that E_{CORR} increases proportionally with log $[H_2O_2]$ for $[H_2O_2]$ <

10^{-4} Mand that above this concentration, E_{CORR} becomes independent of $[H_2O_2]$ [9]. We have also established that under continuous γ-irradiation, $[H_2O_2]$ is roughly proportional to the square root of the dose rate [7]. At our dose rate (4.3 to 5.5 kGy h^{-1}) the concentration of the radiolytically produced $[H_2O_2]$ is ~10^{-4} M at pH 10.6 and 25 °C, so we are very near the limit at which a higher dose rate would have no impact, and we should be able to extrapolate downwards to estimate the effect on E_{CORR} of lower dose rates. We can note that the dose rate to the coolant in the reactor core will be much higher than the fields that we can obtain in our gamma cell while they will be lower (but non-zero) outside of the core. However, H_2O_2 that is generate in the core by radiolysis will persist in the coolant as it is transported out of the core.

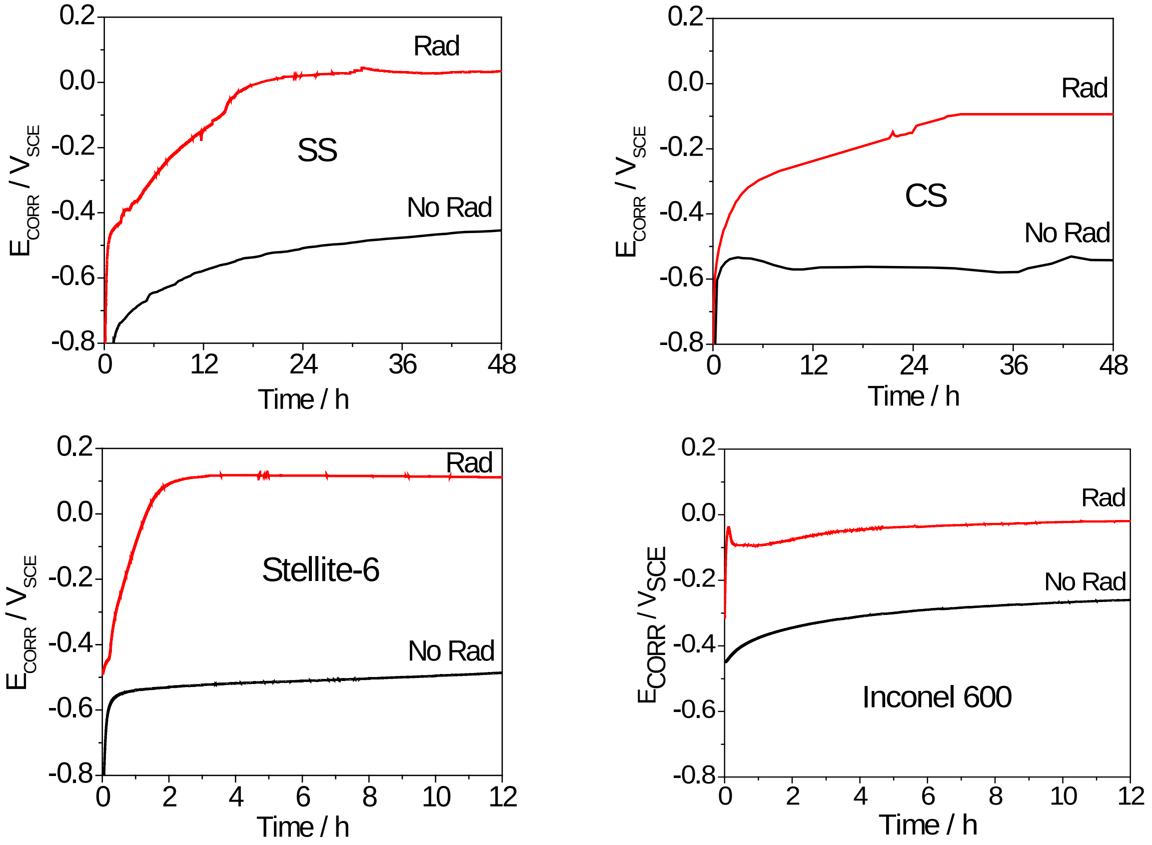

Figure 1: E_{CORR} as a function of time recorded on the alloys with and without γ-irradiation atpH 10.6 and room temperature.

3.2 Oxide Formation as a Function of Potential

The electrochemical reactivity and solubility of the oxide present on an alloy surface are important in determining the net rates of metal oxidation and dissolution. Thus, it is important to determine the type and the thickness of oxide that can be formed as a function of E_{CORR} in order to fully understand the effect of radiation on corrosion behaviour.Since E_{CORR} represents the potential at the electrode surface, we can apply the potential externally, instead of letting the aqueous environment dictate the potential.Thus, oxide formation as a function of applied potential (E_{APP}) has been studied under both potentiodynamic (cyclic voltammetric) and potentiostatic conditions. Cyclic voltammetry was performed primarily to determine the type of electrochemical oxidation that can occur as a function of potential and to aid in the interpretation of the films grown during potentiostatic polarization.The oxide growth under a slowly changing E_{CORR} is better studied under potentiostatic conditions.

The cyclic voltammograms(CVs) obtained for the alloys in deaerated 10 mM borate solutions at pH 10.6 and 25 ^{o}C are shown in Fig. 2.The potential dependent behaviour of the anodic activity (or current) matches the behaviour expected based onthe thermodynamic equilibrium potentials for the redox reactions of the main alloy elements (i.e. Fe, Ni, Co and Cr) at pH10.6 at 25 ^{o}C, as illustrated in Fig. 3[1–3, 9,10]. Thishas allowed us to assign the current peaks in the CVs to the formation of particular oxides and to identify different potential regions (four for SS and Stellite-6, and three for CS and Inconel 600) where formation of certain oxides is favored.These potential regions are indicated in Figs. 2 and 3 as horizontal coloured bars labeled Ox I, II, III and IV. More details on the CV results and their analyses can be found in references [1–3, 9].

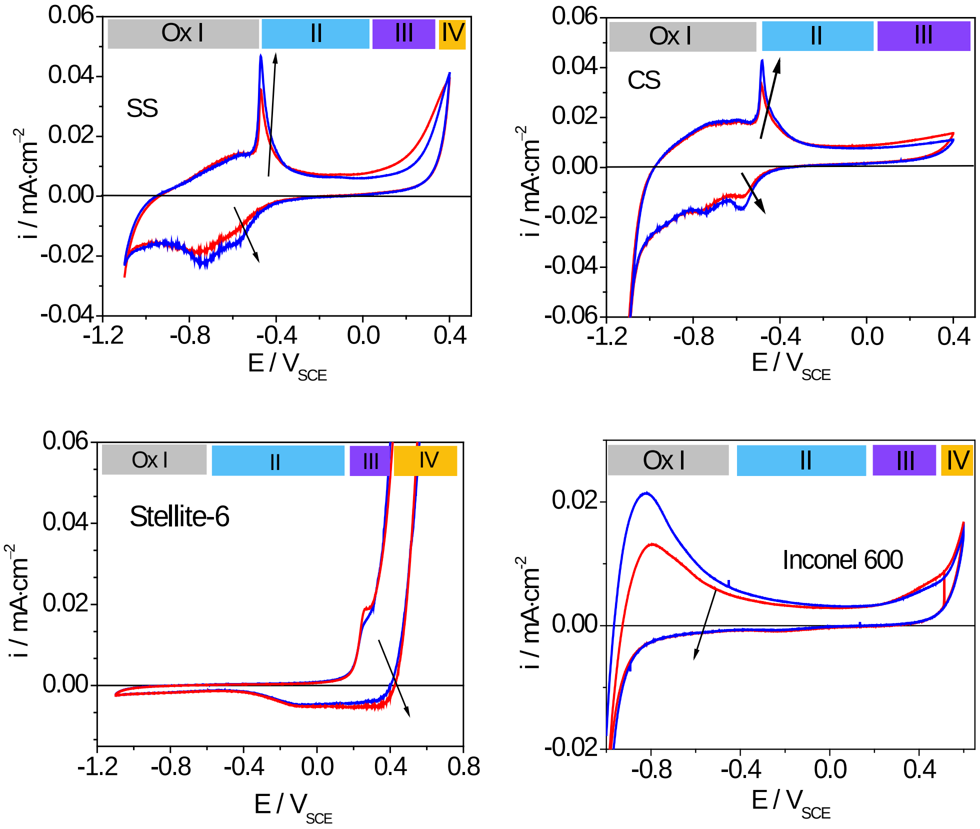

Figure 2: Cyclic voltammograms obtained at pH 10.6 and room temperature. The CVs were recorded at a scan rate.of 5 mV•s$^{-1.}$

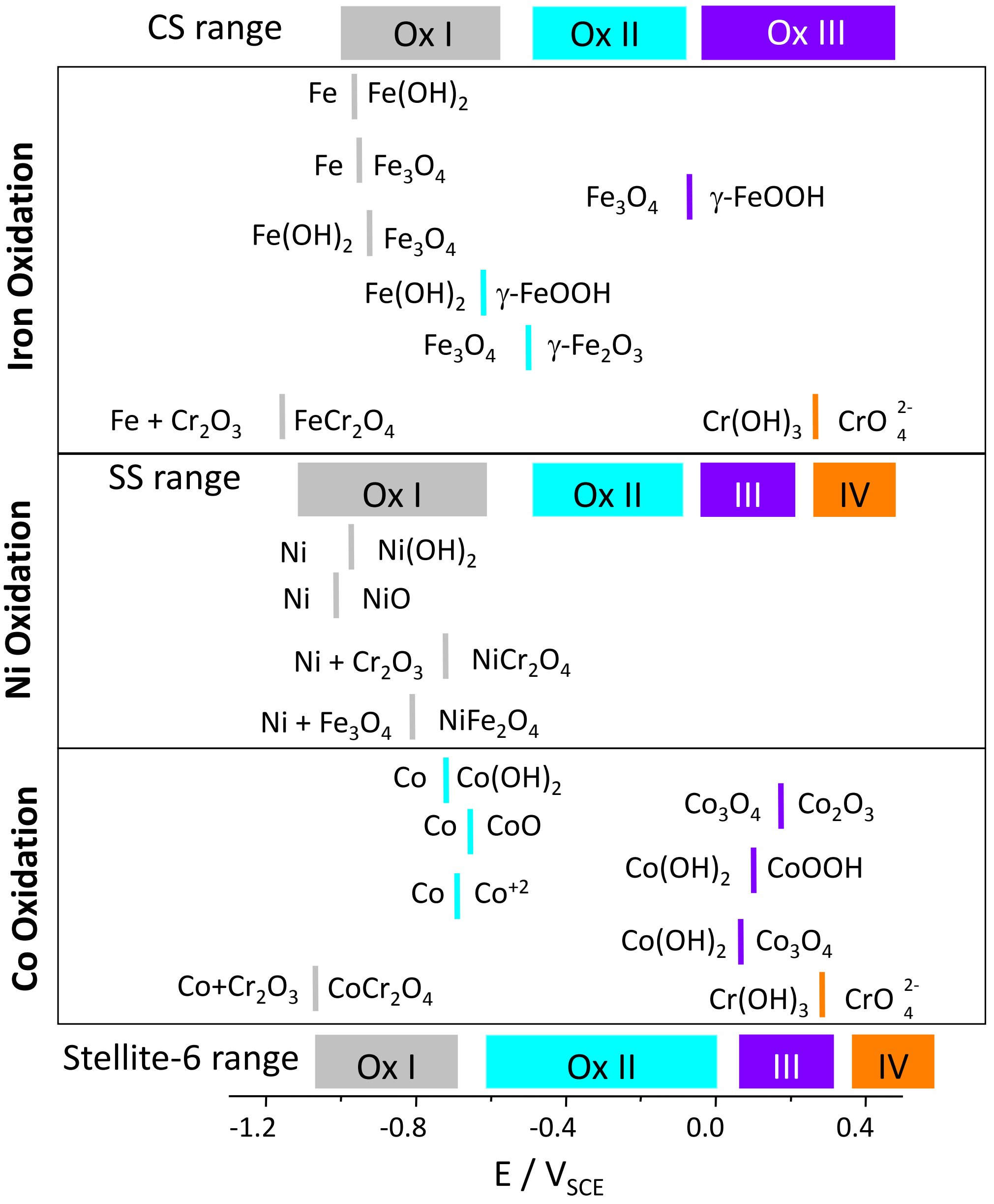

Figure 3: Electrochemical equilibrium potentials for the redox reactions of Cr, Fe, Ni and Co species at pH 10.6 and room temperature. Vertical bars show the equilibrium potentials andthe corresponding redox pairs are listed on both sides of these bars.

The oxide that is formed duringa CV scan is very thin. A thin oxide layer will not suppress subsequent metal oxidation reactions significantly. However, oxide growth and metal dissolution are not only affected by electrochemical reactions but also by non–Faradaic processes such as surface hydration, diffusion, and phase transformation [2,9]. Non-Faradaic processes are independent of electrode potential. Since the type and thickness of oxide that grows affects the potential at the surface and the rates of subsequent electrochemical reactions, non-faradaic processes can indirectly affect the potential–dependent electrochemical reactions. However, long–term potentiostatic studies have shown that the characteristic potential regions determined from the CVs and thermodynamic equilibrium potentials are also useful in determining the nature of the thicker oxide films that grow in each region.

The oxidation regions are based on the potential at the metal/oxide interface. The potential that we measure as E_{CORR} or the potential that we control (E_{APP}) during potentiostatic film growth corresponds to the potential at the oxide/water interface. With a uniform oxide film of finite thickness, the metal oxidation occurs at the metal/oxide interface and the water reduction occurs at the oxide/water interface, as schematically shown in Fig. 4. For the full electrochemical reaction to occur, migration of the metal cation from the metal/oxide interface to the oxide/water interface, or migration of the oxygen anion in the reverse direction is required. The driving force for an electrochemical reaction is the difference in the electrochemical equilibrium potentials of the two half reactions that occur at the two interfaces. With a resistive oxide layer, the potential difference drops from the metal/oxide interface, across the oxide layer to the oxide/water interface (ignoring the potential drop across the double layer in the electrolyte at the water/oxide interface). As illustrated in Fig. 4, this reduces the driving force for the metal oxidation (overpotential, η_{Ox}), that is the potential difference between the potential present at the metal/oxide interface and the equilibrium potential (E_{eq}(M/Ox)) required for the metal oxidation process. Due to the potential drop across the oxide layer, ΔE_{ox}, the potential at the metal/oxide interface is not the same as E_{CORR}. The potential at the metal/oxide interface cannot be directly measured. The value of E_{CORR} provides an upper limit for the potential at the metal/oxide interface and, with some understanding of the conducting properties of the oxide layer present, oxidation reactions, and hence the oxide that can be formed, can be understood.

Based on both the CV and potentiostatic studies,dominant oxide growth mechanisms that occur in the different potential regions have been proposed:

Film Growth in Region Ox I: On CS, the surface is quickly covered by a uniform but insoluble $Fe^{II/III}$ magnetite layer, due to the low iron solubility at pH 10.6, and this oxide grows uniformly. On SS and Inconel 600, the oxidation of Fe to Fe^{II} leads first to the conversion of the pre–existing chromium oxide to a chromite-like oxide ($FeCr_2O_4$). As this chromium oxide layer is saturated with Fe^{II}, the Fe^{II} that reaches the oxide/water interface can be further oxidized to form magnetite.The rate of Fe oxidation is slower on SS and Inconel 600 than on CS because the rate of migration of $Fe^{II}$is slower through a chromium oxide/chromite layer than through a magnetite layer.The rate is slower on Inconel 600 than on SS because Inconel has lessoxidizable Fe available. On Stellite-6, the oxidation of Co to Co^{II} converts a pre-existing chromium oxide layer to cobalt chromite.

Film Growth in Region Ox II: On CS, at this potentialmagnetite formation is faster and the magnetite that is formed is further oxidized to a more maghemite–like phase (γ-Fe_2O_3) near or at the oxide/water interface.The formation of maghemite, which is more insulating than magnetite, suppresses further anodic oxidation and the oxide is thin. On SS and Inconel 600, the oxidative conversion ofchromium oxide to a chromite is achieved quickly and the Fe^{II}that reaches the oxide/water interface can be further oxidized to form γ-FeOOHand/or magnetite and this is then oxidized to maghemite.On Stellite-6, the oxidation of Co to Co^{II}continues. When the outer chromite layer becomes saturated with Co^{II}, CoO/$Co(OH)_2$ is formed at the oxide/water interface.

Film Growth in Region Ox III: On CS, SS and Inconel 600, the layer of magnetite/ maghemite/γ-FeOOH grows rapidly via continuous film fracture and repassivation. The difference between these alloys is that the oxide growthon SS and Inconel 600occurs on top of the chromite layer. The oxide grown in this way is porous and less protective. On Stellite-6, Co^{II}oxide/hydroxide is continuously formed on the cobalt chromite layer and this oxide is also further oxidized to less soluble $Co^{II/III}$ and/or Co^{III}oxides/hydroxides.

Film Growth in Region Ox IV: On SS, Inconel 600 and Stellite-6, the insoluble Cr^{III} oxide can be oxidized to soluble Cr^{VI} species. Depending on how fast this potential is reached the oxidative dissolution of chromium becomes the dominant anodic process. There is no separate Ox IV region for CS.

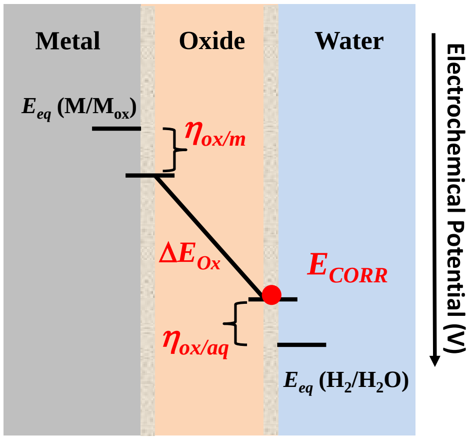

Figure 4: Schematic diagram for corrosion potential, E_{CORR}.

3.3 Effect of γ–Radiation on Oxide Formation.

For all of the alloys studied the steady-state E_{CORR} values in the absence of γ-radiation put the potential at the metal/oxide interfaces near the boundary of Ox I and II. Exposing the system to γ-radiation increases the driving force for the electrochemical reactions and shifts E_{CORR} values to potentials at the metal/oxide (or oxide/oxide) interface to values near the boundary between Ox II and Ox III regions.

To date the effect of γ-radiation on E_{CORR} has been measured only at room temperature. The measurement of E_{CORR} at higher temperatures under intense γ-irradiation is difficult due to the unavailability of a stablereference electrode that can be used under these conditions. We cannot perform direct electrochemical measurements, but we can study the oxides that are formed under those conditions. The combined effect of radiation and temperature on oxide formation on these alloys is being further investigated by analyzing metal coupons corroded with and without irradiation [11,12].

To date these studies have been performed at temperatures up to 150 ^{o}C, but we only discuss results from 80 ^{o}C tests here. A range of surface analyses including X-ray photoelectron spectroscopy (XPS), Auger electron spectroscopy (AES) and Raman spectroscopy were performed on the surfaces to determine the chemical and phase compositions of the oxides formed. These results have been described in detail elsewhere [11, 12].The micrographs of the oxidesformed onCS and SS at 80 ^{o}C, with and without irradiation, are compared with those of oxides formed potentiostaticallyat different oxidation potential regions in Fig. 5. The electrolyte solutions ($pH_{25^{o}C}$ 10.6, deaerated0.01 M borate solutions) used in this study were the same as those used in the room temperature studies presented in Fig. 1 and 2. The SEM images shows evidencethat at 80 ^{o}C, the oxides formed on the alloys without irradiation are very similar to those formed potentiostatically at potentials in Ox I for CS and SS whereas those formed under irradiation are similar to those formed at potentials in Ox II. It can be noticed that the irradiated SS sample surface containsa small quantity of Fe_3O_4 (small dots) and mostlyγ-FeOOH(spear-shaped branches). An XPS analysis of SS films grown in absence of γ-radiation indicates that they are predominantly magnetite and chromite. In presence of γ-radiation, the iron content increases and a large amount of γ-FeOOH is detected[1].Carbon steel samples shows that the oxide film grown in the absence of γ-radiation is mainly Fe_3O_4 while the oxide formed under irradiation consists of γ-Fe_2O_3 grown on top of Fe_3O_4[2,11].

Theshift in E_{CORR} caused by γ-radiation may be beneficial. At pH 10.6, the increase in E_{CORR} due to γ-radiation leads to a more protective oxide film on CS, while it does not appear to offer a similar advantage on SS. Further analysis of the morphology of the oxide films formed on Stellite-6 and Inconel 600 is ongoing.

The potentiostatic film growth as a function of potential can be performed at higher temperatures [2,12]. Temperaturehas a negligible effect on the electrochemical equilibrium potentials for metal oxidation reactions (over the temperature range of interest) and hence, the characteristic potential regions for metal oxidation defined above do not change significantly with temperature [2,12,13].

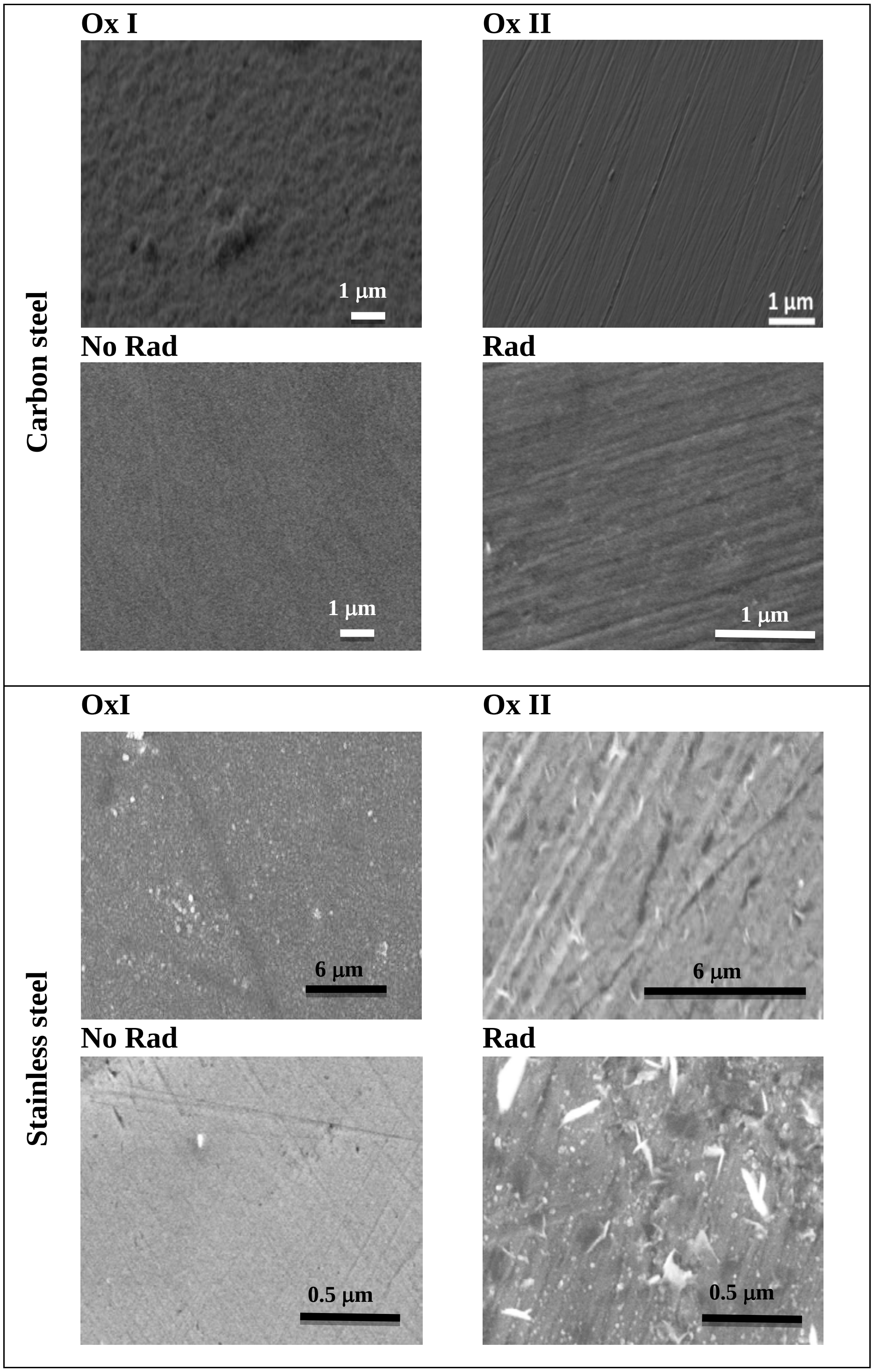

Figure 5:SEM micrographs of samples surfaces obtained potentiostatically at different oxidation regions and those obtained in the absence and presence of γ-radiation in adearated 0.01 M borate solution at 80 °C and pH10.6.

Thus, the type of oxide that can be formed as a function of potential does not change significantly with temperature. Temperature does, however, change the rates of metal oxidation and metal dissolution, thereby affecting the thickness and surface morphology of the oxide film that is grown [2,12,13]. We have observed a small change in $E_{CORR}$with increased temperature [14]. This small change is attributed primarily to the change in the thickness of the oxide layer formed (and the impact of the greater film resistance on the potential at the water/oxide interface).

4. Summary

Ionizing radiation has a major impact on the corrosion process by shifting E_{CORR} to more positive values by producingredox active species (particularly H_2O_2) in the aqueous phase. At our dose rate the concentration of the radiolytically-produced [H_2O_2] is at a level that results in the maximum change in E_{CORR} that can be caused by water radiolysis. The increase in E_{CORR} caused by γ-radiation is enough to put the studied alloys into a different oxidation region where the characteristic oxide that is formed is different.

Depending on the alloy and the water pH, the increase in E_{CORR} may be beneficial. At pH 10.6, an increase in E_{CORR} due to γ-radiation leads to a more protective oxide film on CS, while it does not appear to offer a similar advantage on SS. Further analysis of the oxide films formed on Stellite-6 and Inconel 600 is ongoing, and further tests are in progress to characterize the impact of higher temperatures on oxide formation.

For practical application to a particular nuclear plant, an assessment of the dose rates throughout the reactor cooling circuit and the mass transport of$H_2O_2$from the core would be required to determine the corrosion implications at particular locations in the cooling circuit.

5. Acknowledgement

This research was funded under the Natural Science and Engineering Council of Canada (NSERC) and Atomic Energy of Canada Limited (AECL) Industrial Research Chair in Radiation Induced Processes. The ^{60}Co γ-irradiation cell and the electrochemical analysis equipment were purchased under a grant from the Canada Foundation for Innovation. Surface Science Western is greatly acknowledged for the SEM images.

6. References

[1] Q.W. Knapp, J.C. Wren, “Film formation on Type-316L stainless steel as a function of potential: Probing the role of gamma-radiation”, ElectrochimicaActa, 80, (2012, pp. 90–99.

[2] K. Daub, X. Zhang, L. Wang, J.J. Noel, J.C. Wren, “Oxide growth and conversion on carbon steel as a function of temperature over 25 and 80°C“, ElectrochimicaActa, 56, 2011, pp. 6661–6672.

[3] M. Behazin, M.C. Biesinger, J.J. Noël, J.C. Wren, “Comparative study of film formation on high-purity Co and Stellite-6: Probing the roles of a chromium oxide layer and gamma-radiation”, Corrosion Science, 63, 2012, pp. 40–50.

[4] B. E. Zimmerman, R. Collé, “ Standardization of ^{63}Ni by 4πβ liquid scintillation spectrometry with ^{3}H-standard efficiency tracing”, Journal of Research of the National Institute of Standards and Technology, 102, 1997, pp.455–477.

[5] G. Hirschberg, P. Baradlai, K. Varga, G. Myburg, J. Schunk, P. Tilky, P. Stoddart, “Accumulation of radioactive corrosion products on steel surfaces of VVER type nuclear reactors. I. ^{110m}Ag”, Journal of Nuclear Materials, 265, 1999, pp. 273–284

[6] P. Cohen, “Water coolant technology of power reactors”, American Nuclear Society, 1980

[7] J.M. Joseph, B.S. Choi, P. Yakabuskie, J.C. Wren, A combined experimental and model analysis on the effect of pH and O_2(aq) on gamma-radiolytically produced H_2 and H_2O_2”, Radiation Physical Chemistry, 77, 2008, pp. 1009–1020

[8] L. Wang, K. Daub, Z. Qin, J.C. Wren, “Effect of dissolved ferrous iron on oxide film formation on carbon steel”, ElectrochimicaActa, 76, 2012, pp. 208–217

[9] K. Daub, X. Zhang, J.J. Noel, J.C. Wren, Effects of γ-radiation versus H_2O_2 on carbon steel corrosion”, Electrochim. Acta, 55(2010) 2767–2776.

[10] A. Zahs, M. Spiegel, H.J. Grabke, “Chloridation and oxidation of iron, chromium, nickel and their alloys in chloridizing andoxidizing atmospheres at 400–700°C”, Corrosion Sci., 42,2000, pp.1093–1122

[11] K. Daub, X. Zhang, J.J. Noël, J.C. Wren, “Gamma-radiation-induced corrosion of carbon steel in neutral and mildly basic water at 150°C”,.Corrosion Sci., 53, 2011, pp.11-16

[12] M. Behazin, J.J. Noël, J.C. Wren, “ Temperature dependence of radiation-induced corrosion of Stellite-6 at pH 10.6 “,in the proceedings of 33rd Annual Conference of the Canadian Nuclear Society, Saskatoon , June 10–13 (2012).

[13] A.P.M. Camargo, B.A.F. Previdello, H. Varela, E.R. Gonzalez, “Effect of temperature on the electro-oxidation of ethanol on platinum”, Química Nova, 33, 2010, pp. 2143−2147.

[14] Q. Knapp, K. Daub, A.Y. Musa, J.C. Wren, “Radiation-induced corrosion of 316L stainless steel and carbon steel”, in the proceedings of Nuclear Plant Chemistry Conference, Paris, September 24–28 (2012).